ACS APPLIED MATERIALS & INTERFACES

Research Article

www.acsami.org

An Electrochemical Capacitor Electrode Based on Porous Carbon Spheres Hybrided with Polyaniline and Nanoscale Ruthenium Oxide

Dan Zhao, Xinying Guo, Yue Gao, and Feng Gao*

Laboratory of Optical Probes and Bioelectrocatalysis(LOPAB), Anhui Key Laboratory of Chemo/Biosensing, College of Chemistry and Materials Science, Anhui Normal University, Wuhu 241000, P. R. China

ABSTRACT: Nanoscopic ruthenium oxide (RuO_2)/polyaniline (PANI)/carbon double-shelled hollow spheres (CS) composites, RuO_2/PANI/CS, have been prepared via electro-polymerization of aniline and redox deposition of RuO_2 on the surface of CS. The structures and morphologies of the resulting ternary composites are characterized using scanning electron microscopy (SEM), infrared spectroscopy (IR), energy-dispersive X-ray spectroscopy (EDX). The electrochemical properties of the ternary composites as active electrode materials for electrochemical capacitors have been investigated by different electrochemical techniques including cyclic voltammetry, galvanostatic charge−discharge, and impedance spectroscopy. The results show that the specific capacitance of RuO_2/PANI/CS composites is 531 F g^{-1} at 1 mA cm^{-2} in 1.0 M H_2SO_4 electrolyte, which is higher than many other currently available ternary composites based on RuO_2/PANI. At the same time, the composites display a good rate capability and 70% of the initial specific capacitance is retained with the charge−discharge current density up to 10 mA cm^{-2}.

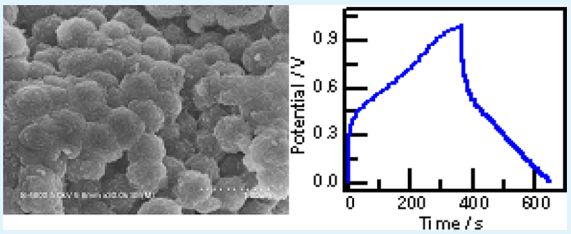

KEYWORDS: *electrochemical capacitors, porous carbon spheres, polyaniline, nanoscopic ruthenium oxide, electropolymerization, redox deposition*

1. INTRODUCTION

Electrochemical capacitors (ECs), also known as supercapacitors, are attractive energy storage devices which store energy using either ion adsorption (electrochemical double layer capacitors, EDLCs) or fast surface redox reactions (pseudocapacitors). ECs combine the advantages of the high power of conventional dielectric capacitors and the high specific energy of rechargeable batteries, and thus show some distinguished merits such as high power density, fairly high energy density, and long cycle life. In recent years, ECs have played an increasing important role in power sources because of the growing demands in digital communications, hybrid electric vehicles, and mobile electronic devices that require electric energy at high power levels in relatively short pulses.[1−5] Presently, the trend in the supercapacitor research is to develop hybrid capacitors with high performance by combining the above-mentioned two different mechanisms.

In the fabrication of ECs, the electrode material is one of the extremely important factors affecting the performance of ECs (energy and power densities, safety, cycle life, etc.).[1,6−8] Carbon-based materials with different forms such as active carbon, carbon fibers, carbon aerogels, carbon xerogels, fullerenes, graphenes, and carbon nanotubes, are attractive electrode materials and have been widely used in ECs due to their chemical stability, and porous nature.[6−18] Carbon materials have been either directly employed as electrodes for electrochemical double layer capacitors,[9−15] or used as electrode matrix to anchor other electroactive materials for pseudocapacitors or hybrid capacitors.[16−21] Although porous carbon materials have high specific surface area, the low conductivity of porous materials limits their applications in high power density supercapacitors.[9−16] To enhance the performances of carbon-based electrochemical capacitors, conducting polymers (e.g., polyaniline, polypyrrole) and metal oxides (e.g., RuO_2, MnO_2, NiO, IrO_2, SnO_2, CoO_x) that undergo fast surface redox (pseudocapacitive) reactions have been employed to be fabricated on carbon matrix.[1,16−21] For instance, as a common conducting polymer, polyaniline (PANI) is generally considered as one of the most intriguing materials for ECs due to its relatively high conductivity, low cost, and easy preparation, and is known to increase the electrochemical capacitance of carbon materials.[22−24] Among these transition metal oxides, ruthenium oxide(RuO_2) has been recognized as one of the most promising electrode materials for ECs and is known to show excellent cycle performance and high specific capacitance.[25−29]

On the basis of the above understanding, the combination of RuO_2 with conducting PANI seems to be a promising attempt to have a possible synergic effect to improve the performances of capacitors. Such investigations were pioneered by Ko et al. who used RuO_2 and polyaniline in combination with Nafion.[30] Recently, RuO_2/PANI composites prepared by chemical oxidation of aniline on RuO_2 attached to the gold substrate in acid media,[31] and PANI/carbon nanotubes/RuO_2 compo-

Received: July 27, 2012
Accepted: September 18, 2012
Published: September 18, 2012

sites via electro-polymerization and electrochemical deposition method[32] have been prepared and used as electrode materials for ECs. Therefore, maximizing utilization of PANI and RuO_2 pseudocapacity and designing highly electrically conductive electrode microstructures are critical to fabricate electrochemical capacitors.

As we know, electrolyte diffusion within the bulk electrode materials is a rate-limiting step. So, optimizing the electrolyte transport paths without sacrificing electron transport is a crucial strategy to improve the rate capacity of ECs. Ordered mesoporous carbon materials are an attractive type with a nanostructured hierarchy with desirable electrolyte transport routes. In our previous studies, we have synthesized a new kind of microstructured porous carbon materials, double-shelled carbon spheres (CS), and have showed excellent electrochemistry properties such as good conductivity, porous nature, high specific area as electrode materials.[33] In this study, PANI/CS composites were synthesized by in situ electro-polymerization of aniline on CS surface, and PANI/CS composites were further employed as matrix material to prepare a RuO_2/PANI/CS composites in which nanoscale RuO_2 was electrodeposited on the PANI/CS matrix surface to produce a thin layer of RuO_2. Using RuO_2/PANI/CS composites as electrode materials, the capacitive performaces have been investigated, and the results demonstrate that the synthesized RuO_2/PANI/CS composites display good conductivity, electrochemical activity, and gravimetric capacitance, outperforming many other currently available carbon-based electrodes.

2. EXPERIMENTAL SECTION

2.1. Chemicals. Aniline and ruthenium(III) chloride hydrate (RuCl3 · 3H2O) were both purchased from Aldrich. N, N-dimethylformamide (DMF), hydrochloric acid (HCl), potassium chloride (KCl), and sulfuric acid (H_2SO_4) were purchased from Sinopharm Chemical Reagent Co. Ltd. (Shanghai, China) and used as received. All solutions were prepared with double-distilled water.

2.2. Synthesis of Carbon Double-Shelled Hollow Spheres (CS). The synthesis of carbon double-shelled hollow spheres was synthesized according to previous literatures.[33] Typically, three steps are involved for the synthesis. First, synthesis of sulfonated polystyrene hollow sphere templates: Freeze-dried polystyrene hollow spheres were immersed in concentrated sulfuric acid at varied temperature and for varied time controlling sulfonation extent. Sulfonation at 40 °C for 1 h results in the sulfonated hollow sphere templates denoted as S1. The sulfonated spheres were thoroughly rinsed with water and ethanol. Second, synthesis of polymer phenolic formaldehyde (PF) composite hollow spheres: The solution of PF resole resin with solid content 60 wt % was prepared by alkaline MgOH catalytic reaction of phenol/formaldehye (molar ratio = 1:1.3). One-tenth of a gram of freeze-dried sulfonated polystyrene hollow sphere template S1 was dispersed in 5 mL of ethanol at ambient temperature. A designed amount of PF resin solution was then dropped into the dispersion under stirring within 10 min followed by a further reaction for 4 h. The weight ratio of phenolic resin and sulfonated polystyrene hollow sphere is chosen 4:1. PF composite hollow spheres were prepared after centrifugation followed by further cross-linking at 150 °C for 2 h. Finally, synthesis of carbon double-shelled hollow spheres: Carbon double-shelled hollow spheres were synthesized by calcination of the phenolic composite hollow spheres at 800 °C for 2 h under nitrogen atmosphere.

2.3. Preparation of CS Film Electrodes. Prior to surface modification, the glassy carbon disk electrodes (GC, 3-mm diameter, Bioanalytical System, Inc.) were first polished with 0.3 and 0.05 μm alumina slurry on a polishing cloth, respectively, and then sonicated in the acetone and distilled water for 3 min, respectively. The as-synthesized CS was dispersed into N,N-dimethylformamide (DMF) to give a homogeneous suspension (10 mg mL^{-1}) under sonication. A 2.0 μL of homogeneous suspension was casted onto the surface of GC electrode and allowed it to dry under lamp to evaporate the solvent, thus a CS-modified GC electrode (denoted as CS/GC electrode) was obtained.

2.4. Preparation of RuO_2/PANI/CS/GC Electrode. PANI and RuO_2 were coated on CS by electropolymerization and electrodeposition methods based on literatures with small modification,[21,35] respectively. PANI was first in situ electropolymerized on CS at a constant potential of 0.75 V for 420 s with CS/GC electrode as working electrode, Pt wire as counter electrode, and Ag/AgCl as reference electrode. The electrolyte was 200 mL of aqueous solution containing 0.5 M H_2SO_4 and 0.05 M aniline. After the deposition of PANI, the PANI/CS/GC electrode was washed with water, following by the deposition of RuO_2. Cyclic voltammetry was employed to deposit hydrous RuO_2 on PANI/CS composite. In a strong acid electrolyte (pH ~2) containing 5 mM $RuCl_3$, 0.01 M HCl, and 0.1 M KCl, RuO_2 was deposited on PANI/CS composite with a scan rate of 50 mV s^{-1} in the potential range from −0.2 to 1.0 V for 120 cycles. After deposition, the electrode was also washed with water and air-dried completely for further use.

2.5. Physical-chemical Characterization and Electrochemical Characterization. The as-prepared electrode materials were characterized by S-4800 field emission scanning electron microscopy (Hitachi, Japan) for morphological measurement, energy dispersive X-ray spectroscopy (EDX) for element analysis, and 8400S FT-IR spectrophotometer (Shimadu, Japan) for IR spectra. Electrochemical measurements were performed on CHI 760D electrochemical workstation (CHI, Shanghai) with a conventional three-electrode, single compartment electrochemical cell which consists of a glass carbon electrode or composite-modified electrode as working electrode, a Ag/AgCl (in 3 M KCl) as reference electrode, and a platinum wire as counter electrode. The electrochemical performances of the prepared electrodes were characterized with cycle voltammetry (CV), electrochemical impedance spectroscopy (EIS), charge−discharge tests. The electrolyte for electrochemical experiments was 1.0 M H_2SO_4. All the experiments were carried out at room temperature. The amount of composite materials modified on electrode surface was obtained form the weight difference before and after loading. The weighting was carried out on a digital Ultramicrobalance balance (Mettler Toledo) with a sensitivity of 1.0 μg. Brunauer−Emmett−Teller (BET) surface area was determined using surface area and porosimetry system (Micromeritics ASAP 2020 M Porosity Analyzer). Conductivity was measured on compressed pieces of dry powders using a standard four-probe method.

3. RESULTS AND DISCUSSION

3.1. Physical-chemical Characterization of Synthesized Electrode Materials. The detailed characterizations of the synthesized carbon sphere including SEM, TEM, IR spectra, element analysis, Raman spectra, and BET test were reported in our previous publication.[33] In summary, the carbon spheres with porous shell are about 480 nm in diameter. BET specific surface area was 194 m^2/g, and the total pore volume was 0.36 cm^3/g. The pores were possibly originated from the release of small molecules and decomposition of the sulfonated polystyrene gel during carbonation. Elemental analysis shows that the carbon spheres contain 94.0 wt % C, 1.0 wt % H, 2.7 wt % O, and 1.0 wt % S, suggesting that oxygen-containing functional groups are present on the CS surface. The SEM images of the synthesized carbon sphere are shown in Figure 1A.

PANI/CS composites were prepared by in situ anodic electropolymerization of aniline monomers on CS/GC electrode impregnated in a mixed solution containing 0.05 M aniline and 0.5 M H_2SO_4. After the electrolyte was deaerated with nitrogen, anodic polymerization of the aniline monomers

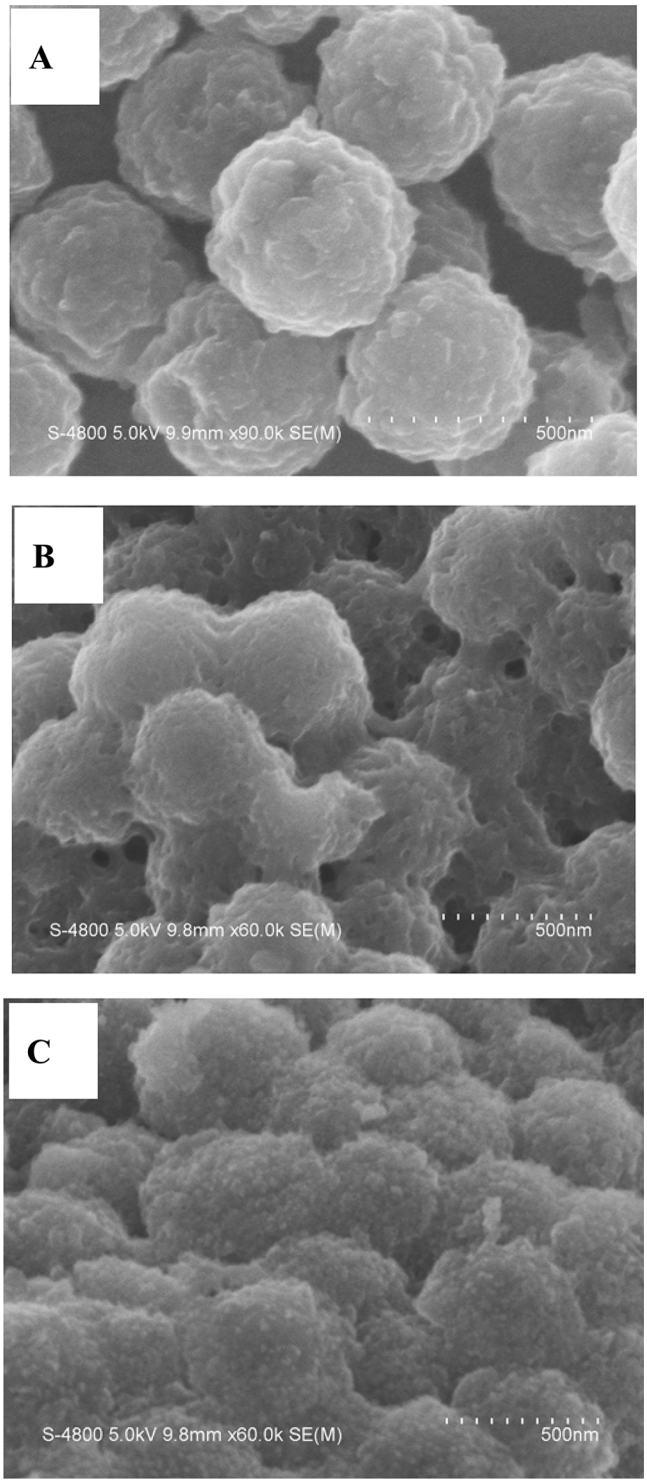

Figure 1. Typical SEM images of (A) carbon sphere (CS), (B) PANI/CS composite, and (C) RuO_2/PANI/CS composite.

was achieved at the working electrode poised with a constant potential of 0.75 V (vs Ag/AgCl reference electrode) for 7 min. The morphology of PANI/CS composites was studied using SEM image. As shown in Figure 1B, a salient morphology change appears on the external surface of carbon spheres, which is attributed to the freshly electro-polymerized PANI. Figure 2 displays the IR spectra of CS, and PANI/CS composites, respectively. Characteristic peaks at 3450, 1625, and 1122 cm^{-1} are observed in the IR spectrum of carbon spheres (curve a).

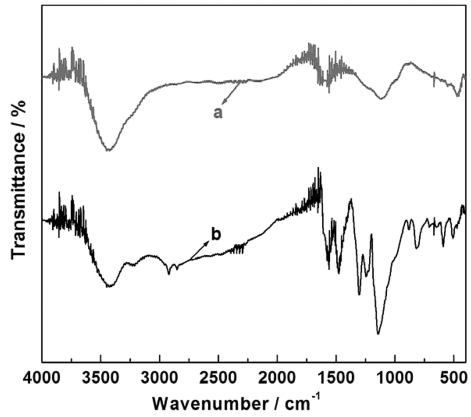

Figure 2. IR spectra of (a) CS and (b) PANI/CS composites.

These peaks can be ascribed to the stretching vibration of −OH, C═O, and C−C−O, respectively.[33] As shown in curve b of Figure 2, the characteristic peaks at 1574 cm^{-1} and 1482 cm^{-1} correspond to the quinoid ring and the benzene ring, respectively. The bands in the range of 1200−1400 cm^{-1} are the C−N stretching band of an aromatic amine. The characteristic band of polyaniline base is the N═Q═N stretching band at 1144 cm^{-1}. These results are good agreement with other publications[23,34] and indicate that polyaniline was successfully deposited onto carbon spheres in our experiment.

To obtain RuO_2/PANI/CS composites, we deposited RuO_2 on PANI/CS composites using cyclic voltammetry performed in a electrolyte containing 5 mM $RuCl_3$, 10 mM HCl, and 100 mM KCl with a scan rate of 50 mV s^{-1} for 120 cycles in the potential window from −0.2 to 1.0 V (vs Ag/AgCl). The surface morphology of RuO_2/PANI/CS composites was examined by SEM and the typical image is shown in Figure 1C. It is clear that a thinner RuO_2 deposite layer is observed on the surface of PANI/CS composite matrix. The thinner deposit is very rough, on which many spherical grains with various sizes of several tens of nanometers are observed. Figure 3 displays the energy-dispersive X-ray spectra (EDX) and the result further confirm that RuO_2 has been successfully deposited onto PANI/CS composite matrix.[17,34]

3.2. Electrochemical Characterization of Synthesized Electrode Materials. To evaluate the electrochemical capacitance characteristics of the prepared materials including

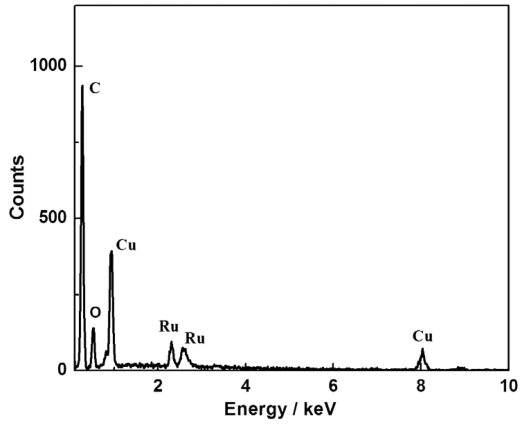

Figure 3. EDX patterns for RuO_2/PANI/CS composites.

dx.doi.org/10.1021/am301484s | ACS Appl. Mater. Interfaces 2012, 4, 5583−5589

CS, PANI/CS, and RuO_2/PANI/CS, we performed cyclic voltammetry (CV) and charge tests. Figure 4 illustrates the CV

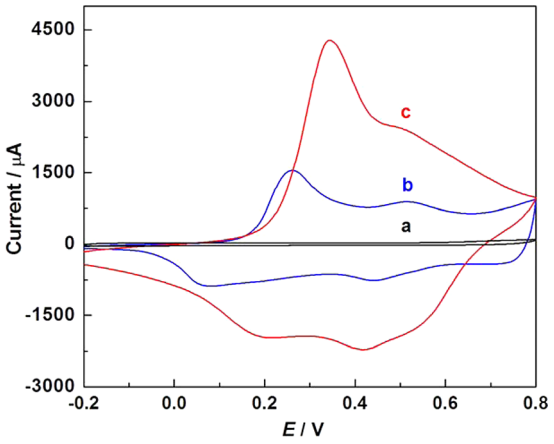

Figure 4. Cyclic voltammograms of (a) CS (black line), (b) PANI/CS (blue line), and (c) RuO_2/PANI/CS (red line) modified GC electrodes recorded in deoxygenated 1 M H_2SO_4 with a scan rate of 50 mV s^{-1}.

curves of CS/GC, PANI/CS/GC, and RuO_2/PANI/CS/GC electrodes in the potential range from −0.2 to 0.8 V in deoxygenated 1.0 M H_2SO_4 at a scan rate of 50 mV s^{-1}, respectively. As shown in Figure 4a, CS/GC electrode displays the capacitance characteristic of the electric double layer capacitance, which would produce a CV curve close to the ideal rectangular shape. Figure 4b shows the CV of PANI/CS/GC electrode and two couples of redox peaks are observed. The two couples of redox peaks are attributed to the redox transition of PANI between a semiconducting state (leucoemeraldine form) and a conducting sate (polaronic emeraldine form), and between emeraldine salt and pernigraniline, respectively.[23,34] The redox processes of PANI produce the pseuocapacitance of the PANI/CS/GC electrode.[23,34] After the deposition of RuO_2 on PANI/CS matrix, the current in the plateau region is higher than that of PANI/CS/GC electrode, as shown in Figure 4c. The higher current level implies a larger electrode capacitance. The relationship between peak currents and scan rates has been investigated at RuO_2/PANI/CDS electrode and the plot is shown in Figure 5. As shown in this

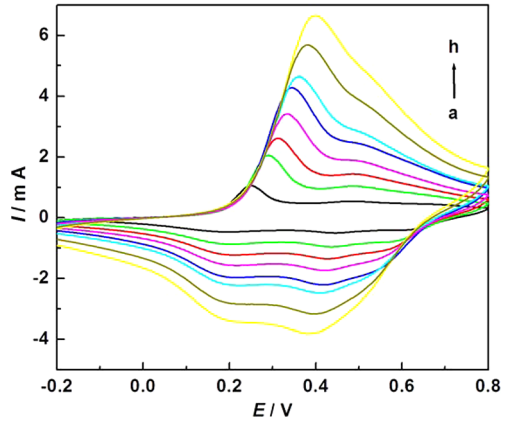

Figure 5. Cyclic voltammograms of RuO_2/PANI/CS/GC electrode at different scan rates (from a to h: 10, 20, 30, 40, 50, 60, 80, 100 mV s^{-1}) in 1 M H_2SO_4 electrolyte.

figure, the redox currents of the RuO_2/PANI/CS/GC electrode increase clearly with the increasing of scan rates, indicating its good rate ability of the electrode. It should also be noted that with the increasing scan rates, a positive shift of oxidation peaks and a negative shift of reduction peaks are observed, which is mainly due to the resistance of the electrode.

The galvanostatic charge−discharge curves of PANI/CS, RuO_2/CS, and RuO_2/PANI/CS composite electrode examined in 1 M H_2SO_4 electrolyte at a current density of 1 mA cm^{-2} are

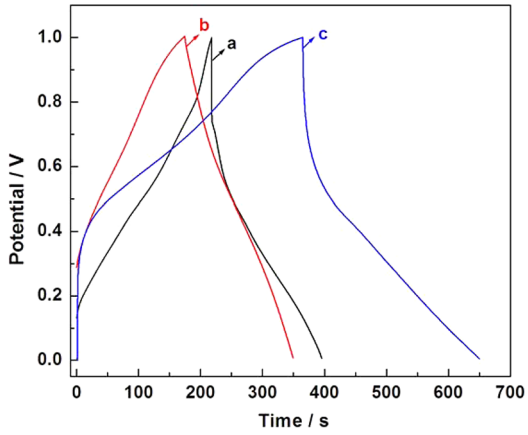

Figure 6. Galvanostatic charge−discharge curves of (a) PANI/CS, (b) RuO_2/CS, and (c) RuO_2/PANI/CS composite electrodes at a current density of 1 mA cm^{-2} in 1 M H_2SO_4 electrolyte. Mass of the active material in every sample: 0.04 mg.

shown in Figure 6. The specific capacitance (C_m) can be calculated according to the following equation[2,3]

$$C_m = \frac{C}{m} = \frac{I\Delta t}{\Delta V m}$$

Herein, C_m is the specific capacitance (F g^{-1}), I is the charge−discharge current, Δt is the discharge time, ΔV is the electrochemical window (1.0 V), and m is the mass of active material within the electrode (0.04 mg). The specific capacitances of PANI/CS, RuO_2/CS, and RuO_2/PANI/CS composite calculated from Figure 6 were 248, 412, and 531 F g^{-1} at 1 mA cm^{-2}, respectively. The specific capacitance obtained at the resultant ternary RuO_2/PANI/CS composite electrode is higher than that obtained at other ternary composites based on RuO_2/PANI, for example, 475 F g^{-1} for PANI/Nafion/RuO_2,[30] and 441 F g^{-1} for PANI/CNT/RuO_2.[32] The high specific capacitance of RuO_2/PANI/CS could be attributed to the novel structure with large surface and high conductive nature in the electrode composites which can provide good electronically conducting pathways for both protonic and electronic transportation during the rapid charge/discharge process. The Brunauer−Emmett−Teller (BET) surface area and the electron conductivity of these three samples were measured. The BET specific surface area values are 194, 159, and 316 m^2/g for CS, PANI/CS, and RuO_2/PANI/CS, respectively. Conductivity was measured on compressed pieces of dry powders using a standard four-probe method at room temperature, and the electron conductivity values for CS, PANI/CS, and RuO_2/PANI/CS are 1.5×10^{-2}, 1.1×10^{-2}, and 2.9×10^{-1} S cm^{-1}, respectively.

Figure 7 shows the charge−discharge curves of the RuO_2/PANI/CS composite electrodes at different current densities,

dx.doi.org/10.1021/am301484s | ACS Appl. Mater. Interfaces 2012, 4, 5583−5589

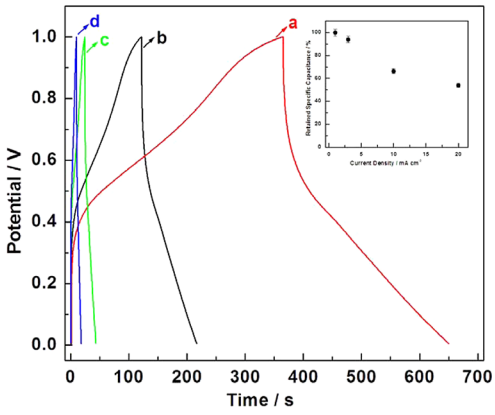

Figure 7. Galvanostatic charge–discharge curves of RuO_2/PANI/CS composite electrode at a current density of 1, 3, 10, 20 mA cm^{-2} in 1 M H_2SO_4 electrolyte. Insert: The relation between the specific capacitance obtained at different current density at the RuO_2/PANI/CS composite electrode. Mass of the active material in every sample: 0.04 mg.

and the relation between the specific capacitance and discharging current of the RuO_2/PANI/CS composite electrode obtained from charging-discharging measurements at different current densities are shown in Figure 7 as an inset. As the current density is increased from 1 to 10 mA cm^{-2}, ca. 70% of the capacitance of the composite electrode is retained, while the current density is further increased to 20 mA cm^{-2}, ca. 54% of the capacitance is still retained. These results indicate a good rate capability of the capacitance electrode. A good rate capability is indicative of high power density.

The energy density (E_m) of the supercapacitor can be calculated using the following equation[2]

$$E_m = \frac{1}{2} C_m (\Delta V)^2$$

The specific power density (P_m) of the supercapacitor can be calculated according to the following equation[2]

$$P_m = \frac{P}{m} = \frac{I\Delta V}{m}$$

where C_m is the specific capacitance, I is the current of charge–discharge, ΔV is the potential range of a supercapacitor (1.0 V), and m is mass of active materials (0.04 mg). The energy density and power density of RuO_2/PANI/CS composite electrode were calculated to be 73.8 Wh kg^{-1} and 1.8 kW kg^{-1} at 1 mA cm^{-2}, respectively. The power and energy-storage capabilities of an electrode are related in the specific power vesus specific energy characteristics of the electrode. Such characteristics for the RuO_2/PANI/CS composite electrode are plotted in Figure 8. The characteristics indicate that the RuO_2/PANI/CS composite electrode has a superior performance in terms of power capability and stored energy.

Charge–discharge measurements are critical in the analysis and prediction of the active materials performance under practical operating conditions. The cycling stability of the RuO_2/PANI/CS composite electrode was examined in 1 M H_2SO_4 aqueous electrolyte by repeating charge–discharge test at a current density of 1 mA cm^{-2}, as shown in Figure 9A. Figure 9B showed that the discharge capacitance loss was about 4% of the initial value after 100 consecutive cycles, 8% after 500 consecutive cycles, 11% after 1000 consecutive cycles, and 27% after 1500 consecutive cycles. This cycling performance is

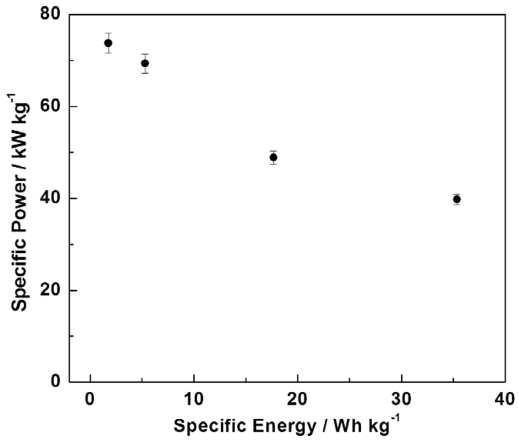

Figure 8. Plot for specific power against specific energy characteristics of the RuO_2/PANI/CS composite electrode.

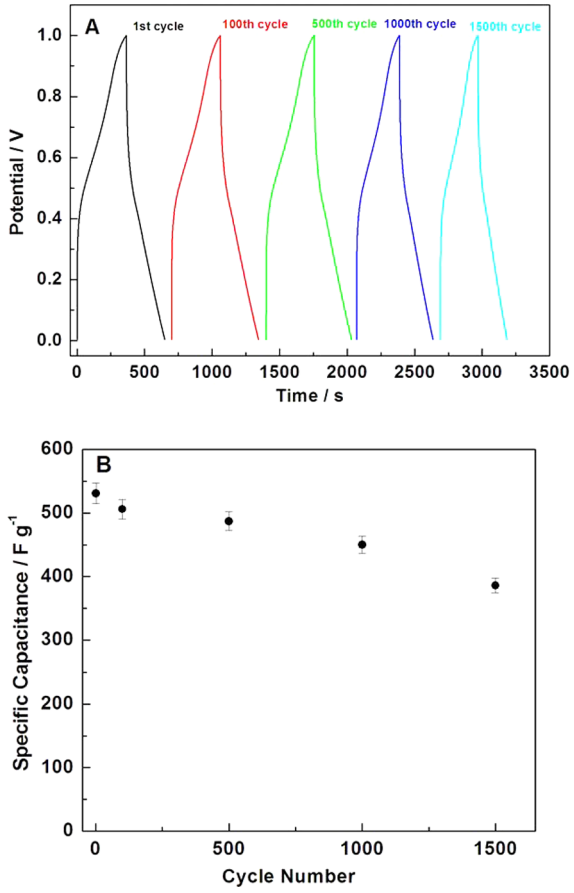

Figure 9. (A) Charge–discharge curves, and (B) specific capacitance of the RuO_2/PANI/CS composite electrode as a function of cycling numbers at a current density of 1 mA cm^{-2}. Mass of the active material in every sample: 0.04 mg.

comparable or prior to some other electrode materials of electrochemical capacitors, such as RuO_2/TiO_2 nanofibre electrochemical capacitor in aqueous 0.5 M H_2SO_4 solution (7% loss after 300 cycles),[26] α-MnO_2-graphene electrochemical capacitor in Na_2SO_4 solution (21% loss after 1000 cycles),[36] PANI/CNT/RuO_2 in 1.0 M H_2SO_4 solution (12.5% loss after 1000 cycles),[32] and MnO_2/MWCNT composite (27.7% loss after 300 cycles).[37] These results indicate that both the as-prepared composite materials have got good cycle stability and

dx.doi.org/10.1021/am301484s | ACS Appl. Mater. Interfaces 2012, 4, 5583–5589

fairly high degree of reversibility in the repetitive charge–discharge cycling.

Electrochemical impedance spectroscopy (EIS) measurements can provide useful information about the redox reaction resistance and equivalent series resistance. In this study, impedance measurements were carried out to prove the capacitive performances of the RuO_2/PANI/CS composite electrode at a dc bias of 5 mV over the frequency range from 0.01 to 1×10^5 Hz. Figure 10 presents the typical Nyquist plots

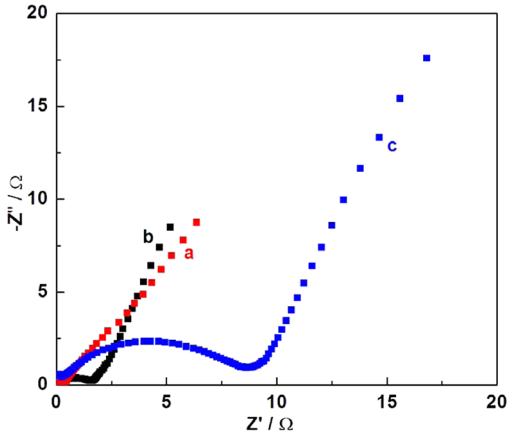

Figure 10. Nyquist plots of (a) CS, (b)RuO_2/PANI/CS, and (c)PANI/CS composites electrodes in 1 M H_2SO_4 electrolyte.

of CS (curve a, red line), PANI/CS (curve c, blue line), and RuO_2/PANI/CS composite electrode in 1 M H_2SO_4 electrolyte, respectively. As shown in this figure, the unequal semicircular can be observed in the high-frequency region. It is apparent that the electrochemical capacitor resistance of CS (curve a, red line) increases significantly to 8.75 Ω (curve c, blue line) with the agglomeration of PANI because of the lower conductivity of PANI. After the loading of RuO_2, the conductivity of the composites is increased and therefore the radius of the semicircular is decreased (curve b, black line). In the low-frequency region, the impedance plot of RuO_2/PANI/CS composite electrode exhibits a nearly straight line of a limiting diffusion process, which is a characteristic feature of pure capacitive behavior.[38]

The maximum power density (P_{max}) of the capacitor is calculated from the following equation[1,2]

$$P_{max} = \frac{V^2}{4Rm}$$

Where V is the cell voltage (here it is 1 V), R is the equivalent series resistance (ESR) measured with impedance spectra at the low-frequency region, and m is the total mass of active materials of both electrodes (in this case m = 8 mg). In this study, the maximum power density (P_{max}) of the capacitor is calculated to be 20.8 kW kg^{-1}. This value of power density is well-suited for surge-power delivery applications.[15]

4. CONCLUSION

In this paper, the RuO_2/PANI/CS composites were prepared by coimmobilizing PANI and RuO_2 on the surface of porous double-shelled carbon spheres. The electrochemical properties of the composites as active electrode materials for electrochemical capacitors were investigated by different electrochemical techniques including cyclic voltammetry, galvanostatic charge–discharge, and electrochemical impedance spectroscopy. The results showed that the specific capacitance of RuO_2/PANI/CS composites was 531 F g^{-1} at 1 mA cm^{-2}. At the same time, the composite displayed a good rate capability and 70% of the initial specific capacitance was retained with the charge–discharge current density up to 10 mA cm^{-2}. We also believe that the synthesized carbon spheres could serve as a scaffold for other transition-metal oxides as well as conducting polymers.

AUTHOR INFORMATION

Corresponding Author

*Tel.: +86-553-3937136. Fax: +86-553-3869302. E-mail: fgao@mail.ahnu.edu.cn.

Notes

The authors declare no competing financial interest.

ACKNOWLEDGMENTS

We are grateful for the financial support from the Natural Science Foundation of China (Grant 21175002), Anhui Provincial Natural Science Foundation for Distinguished Youth (Grant 1108085J09), and the project sponsored by SRF for ROCS, SEM. We also give our deep thanks to Mu Yang, Zhenzhong Yang, and Lanqun Mao of Institute of Chemistry, Chinese Academy of Sciences for their helpful discussions and some assistance in characterization experiments.

REFERENCES

(1) Simon, P.; Gogotsi, Y. *Nat. Mater.* **2008**, *7*, 845–854.
(2) Conway, B. E. In *Electrochemical Supercapacitors: Scientific Fundamentals and Technological Applications*, 1st ed.; Kluwer Academic/Plenum Publishers: New York, 1999, p13–15.
(3) Kötz, R.; Carlen, M. *Electrochim. Acta* **2000**, *45*, 2483–2498.
(4) Burke, A. *J. Power Sources* **2000**, *91*, 37–50.
(5) Ashtiani, C.; Wright., R.; Hunt, G. *J. Power Sources* **2006**, *154*, 561–566.
(6) Zhang, Y.; Feng, H.; Wu, X. B.; Wang, L. Z.; Zhang, A. Q.; Xia, T. C.; Dong, H. C.; Li, X. F.; Zhang, L. S. *Int. J. Hydrogen Energy* **2009**, *34*, 4889–4899.
(7) Inagaki, M.; Konno, H.; Tanaike, O. *J. Power Sources* **2010**, *195*, 7880–7903.
(8) Wu, F.; Xu, B. *New Carbon Mater.* **2006**, *21*, 176–184.
(9) Itoi, H.; Nishihara, H.; Kogure, T.; Kyotani, T. *J. Am. Chem. Soc.* **2011**, *133*, 1165–1167.
(10) Lu, W.; Qu, L.; Henry, K.; Dai, L. *J Power Sources* **2009**, *189*, 1270–1277.
(11) Huang, H. C.; Huang, C. W.; Hsieh, C. T.; Kuo, P. L.; Ting, J. M.; Teng, H. *J. Phys. Chem. C* **2011**, *115*, 20689–20695.
(12) Wang, L. J.; Li, C. Z.; Gu, F.; Zhang, C. X. *J. Alloys Compd.* **2009**, *473*, 351–355.
(13) Calvo, E. G.; Ania, C. O.; Zubizarreta, L.; Menéndez, J. A.; Arenillas, A. *Energy Fuels* **2010**, *24*, 3334–3339.
(14) Lu, W.; Hartman, R.; Qu, L.; Dai, L. *J. Phys. Chem. Lett.* **2011**, *2*, 655–660.
(15) Wang, Y.; Shi, Z. Q.; Huang, Y.; Ma, Y. F.; Wang, C. Y.; Chen, M. M.; Chen, Y. S. *J. Phys. Chem. C* **2009**, *113*, 13103–13107.
(16) Wei, W.; Cui, X.; Chen, W.; Ivey, D. G. *Chem. Soc. Rev.* **2011**, *40*, 1697–1721.
(17) Rakhi, R. B.; Cha, D.; Chen, W.; Alshareef, H. N. *J. Phys. Chem. C* **2011**, *115*, 14392–14399.
(18) Sassin, M. B.; Chervin, C. N.; Rolison, D. R.; Long, J. W. *Acc. Chem. Res.* **2012**, DOI: 10.1021/ar2002717.
(19) Lee, B. J.; Sivakkumar, S. R.; Ko, J. M.; Kim, J. H.; Jo, S. M.; Kim, D. Y. *J. Power Sources* **2007**, *168*, 546–552.
(20) Lee, S. W.; Junhyung Kim, J.; Chen, S.; Hammond, P. T.; Shao-Horn, Y. *ACS Nano* **2010**, *4*, 3889–3896.

(21) Wang, D. W.; Li, F.; Zhao, J.; Ren, W.; Chen, Z. G.; Tan, J.; Wu, Z. S.; Gentle, I.; Lu, G. Q.; Cheng, H. M. *ACS Nano* **2009**, *3*, 1745−1752.
(22) Jiang, J. *Adv. Polym. Sci.* **2006**, *199*, 189−259.
(23) Wang, Y. G.; Li, H. Q.; Xia, Y. Y. *Adv. Mater.* **2006**, *18*, 2619−2623.
(24) Fan, L. Z.; Hu, Y. S.; Maier, J.; Adelhelm, P.; Smarsly, B.; Antonietti, M. *Adv. Funct. Mater.* **2007**, *17*, 3083−3087.
(25) Hu, C. C.; Huang, Y. H. *J. Electrochem. Soc.* **1999**, *146*, 2465−2471.
(26) Ahn, Y. R.; Song, M. Y.; Jo, S. M.; Park, C. R.; Kim, D. Y. *Nanotechnology* **2006**, *17*, 2865−2869.
(27) Gujar, T. P.; Shinde, V. R.; Lokhande, C. D.; Kim., W.-Y.; Jung, K.-D.; Joo, O.-S. *Electrochem. Commun.* **2007**, *9*, 504−510.
(28) Hu, Y. S.; Guo, Y. G.; Sigle, W.; Hore, S.; Balaya, P.; Maier, J. *Nat. Mater.* **2006**, *5*, 713−717.
(29) Barbieri, O.; Hahn, M.; Foelske, A.; Kötz, R. *J. Electrochem. Soc.* **2006**, *153*, A2049−A2054.
(30) Song, R. Y.; Park, J. H.; Sivakkumar, S. R.; Kim, S. H.; Ko, J. M.; Park, D.-Y.; Jo, S. M.; Kim, D. Y. *J. Power Sources* **2007**, *166*, 297−301.
(31) Sopčić, S.; Roković, M. K.; Mandić, Z.; Inzelt, G. J. *Solid State Electrochem.* **2010**, *14*, 2021−2026.
(32) Ko, J. M.; Ryu, K. S.; Kim, S.; Kim, K. M. *J. Appl. Electrochem.* **2009**, *39*, 1331−1337.
(33) Gao, F.; Guo, X.; Yin, J.; Zhao, D.; Li, M.; Wang, L. *RSC Adv.* **2011**, *1*, 1301−1309.
(34) Mi, H.; Zhang, X.; Ye, X.; Yang, S. *J. Power Sources* **2008**, *176*, 403−409.
(35) Liu, F. J. *Polym. Compos.* **2009**, *30*, 1473−1479.
(36) Wu, Z. S.; Ren, W.; Wang, D. W.; Li, F.; Liu, B.; Cheng, H. M. *ACS Nano* **2010**, *4*, 5835−5842.
(37) Wang, H. Q.; Li, Z. S.; Huang, Y. G..; Li, Q. Y.; Wang, X. Y. *J. Mater. Chem.* **2010**, *20*, 3883−3889.
(38) Frackowiak, E.; Delpeux, S.; Jurewicz, K.; Szostak, K.; Cazorla-Amoros, D.; Beguin, F. *Chem. Phys. Lett.* **2002**, *361*, 35−41.